Published online 9 April 2018

Nucleic Acids Research, 2018, Vol. 46, No. 10 ***5061–5074***
doi: 10.1093/nar/gky245

Histone H3 lysine 36 methyltransferase mobilizes NER factors to regulate tolerance against alkylation damage in fission yeast

Kim Kiat Lim[1], Thi Thuy Trang Nguyen[1], Adelicia Yongling Li[1], Yee Phan Yeo[1] and Ee Sin Chen[1,2,3,*]

[1]Department of Biochemistry, Yong Loo Lin School of Medicine, National University of Singapore, Singapore, [2]National University Health System, Singapore and [3]NUS Graduate School for Integrative Sciences & Engineering, National University of Singapore, Singapore

Received March 27, 2017; Revised March 17, 2018; Editorial Decision March 21, 2018; Accepted March 22, 2018

ABSTRACT

The Set2 methyltransferase and its target, histone H3 lysine 36 (H3K36), affect chromatin architecture during the transcription and repair of DNA double-stranded breaks. Set2 also confers resistance against the alkylating agent, methyl methanesulfonate (MMS), through an unknown mechanism. Here, we show that *Schizosaccharomyces pombe* (*S. pombe*) exhibit MMS hypersensitivity when expressing a *set2* mutant lacking the catalytic histone methyltransferase domain or a *H3K36R* mutant (reminiscent of a *set2*-null mutant). Set2 acts synergistically with base excision repair factors but epistatically with nucleotide excision repair (NER) factors, and determines the timely nuclear accumulation of the NER initiator, Rhp23, in response to MMS. Set2 facilitates Rhp23 recruitment to chromatin at the *brc1* locus, presumably to repair alkylating damage and regulate the expression of *brc1*$^{+}$ in response to MMS. Set2 also show epistasis with DNA damage checkpoint proteins; regulates the activation of Chk1, a DNA damage response effector kinase; and acts in a similar functional group as proteins involved in homologous recombination. Consistently, Set2 and H3K36 ensure the dynamicity of Rhp54 in DNA repair foci formation after MMS treatment. Overall, our results indicate a novel role for Set2/H3K36me in coordinating the recruitment of DNA repair machineries to timely manage alkylating damage.

INTRODUCTION

Cells are constantly exposed to internal and external assaults that threaten the integrity of the genome. Inside the cell, DNA damage arises because of errors in replication and transcription, and the persistence of metabolic byproducts, such as reactive oxygen species (ROS) (1). This is compounded by external sources of damage, such as constant exposure to ultraviolet (UV) radiation from sunlight, ionizing radiation, and treatment with certain chemical agents, such as methyl methanesulfonate (MMS) (2,3). MMS is an alkylating, chemotherapeutic agent that induces damage and DNA breaks. If left unrepaired, DNA damage can accumulate, causing instability in the genome and even cell death (4). To defend against these deleterious effects, eukaryotes are endowed with an extensive DNA damage response (DDR) network of proteins that sense and locate the damage, transduce and amplify the emergency signals, and activate specific responses through a coordinated sets of effector proteins (5,6).

The prompt detection of DNA damage is critical for maintaining genomic integrity, with one or more types of DNA damage sensors acting simultaneously. The MRE11-RAD50-NBS1 (MRN) complex (Rad32-Rad50-Nbs1 in *Schizosaccharomyces pombe*) recruits and activates the checkpoint kinase ataxia telangiectasia mutated (ATM; Tel1 in *S. pombe*) at sites of double-stranded breaks (DSBs) via its DSB unwinding and nucleolytic activities (7–9). On the other hand, replication protein A (RPA), which binds the single-stranded DNA (ssDNA), recruits ATM and Rad3-related (ATR; Rad3 in *S. pombe*) via ATR-interacting partner (ATRIP; Rad26 in *S. pombe*) (10,11). ATR responds to DSB signals during DNA replication, whereas ATM responds to various causes of DNA damage as well as the presence of replication adducts at stalled replication forks (12). Working alongside the ATR–ATRIP complex is the PCNA-like sliding clamp loader 9–1–1 complex, comprising Rad9, Rad1, and Hus1, which senses 3′ overhangs generated by the endonuclease cleavage of Mre11 and activates downstream effector proteins at S (Mrc1-Cds1) and G2/M (Crb2-Chk1) checkpoints to halt cell cycle progression in conjunction with regulators that downregulate the

*To whom correspondence should be addressed. Tel: +65 6516 5616; Email: bchces@nus.edu.sg

mitotic transition by cyclin-dependent kinases (CDKs) (13–17).

Appropriate DNA repair mechanisms are activated after DNA damage checkpoint activation to resolve and remove DNA damage. DSBs are the most deleterious type of damage, repaired primarily by two major mechanisms: error-free homologous recombination (HR) or error-prone, non-homologous end joining (NHEJ). HR uses homologous sister chromatids as a template to restore the original sequence at the damaged site, repairing the ssDNA overhang generated by DNA strand resection. Rad51 coats and stabilizes the ssDNA while the Rad54-Rdh54 and Rad55-Rad57 complexes further direct the ssDNA onto complementary sequences (18,19). In comparison, NHEJ is mediated via the direct ligation of broken DNA and is activated by binding of a KU70-KU80 heterodimer, which subsequently recruits DNA-dependent protein kinase (DNA-PKcs) and the DNA ligase IV-XRCC (Lig4/Xlf1 in *S. pombe*) complex (20–22).

Arguably, the most common form of DNA damage is the formation of DNA adducts, which aberrantly distort DNA helices. These adducts form following exposure to agents such as UV radiation and alkylating agents, such as MMS, which covalently modifies DNA bases through methylation, resulting in N7-methylguanine (7-meG) and N3-methyladenine (3-meA). These modified bases are removed by DNA glycosylases through base excision repair (BER), and abasic sites are cleaved by AP endonucleases (for example, Apn2 in *S. pombe*) and AP lyases (for example, Nth1 in *S. pombe*) (23,24). 3-meA and other bulky DNA adducts (e.g., UV-induced pyrimidine dimers) and DNA crosslinks, are also repaired by nucleotide excision repair (NER) machinery (25,26).

NER is mediated via two sub-pathways—transcription-coupled repair (TCR) and global genome repair (GGR)—depending on the mode of damage sensing and DNA strand (25,26). GGR operates throughout the genome, safeguarding transcriptionally inactive regions on both the sense and anti-sense strands. The lesions are first sensed by the damaged DNA-binding (DDB) complex (functional homolog, Rhp7-Rhp16 in *S. pombe*) (27). Conversely, TCR is activated when a lesion is encountered by RNA polymerase II (RNAPII) on the transcribed strand. The stalled RNAPII then recruits Cockayne syndrome A and B (CSA and CSB) proteins (*S. pombe* Ckn1 and Rhp26, respectively) (28,29), which differentially regulate the recruitment of chromatin remodeling and repair factors; although, a recent study has reported CSB-independent TCR in budding yeast involving the Rpb9 subunit of RNAPII and the Sen1 helicase (human senataxin) (30,31).

After sensing damage, GGR and TCR pathways then converge, recruiting the hHR23B-xeroderma pigmentosum (XP) type C (XPC) complex (Rhp23-Rhp41 complex in *S. pombe*) and transcription factor (TF)-IIH, part of the RNAPII preinitiation complex, which unwind the DNA at the site of damage to recruit RPA and XP type A (XPA; Rhp14 in *S. pombe*) proteins (32). These proteins stabilize the opened DNA structure, which is necessary for incision by the endonucleases XPF-ERCC1 (Rad16-Swi10) and XPG (Rad13) (33). Finally, the gap is filled by DNA polymerase δ or ε in conjunction with the clamp loader PCNA-RFC complexes, and the nick is ligated by DNA ligases Lig1 and Lig3 (Cdc17 and Adl1) (34,35).

Recently, the histone H3K36 methyltransferase Set2 has emerged as a key factor in coordinating the DDR, linking DNA damage sensing and repair. In fission yeast, the *set2* null mutant is hypersensitive to numerous DNA damaging agents, including several S-phase disrupting drugs, such as hydroxyurea (HU), MMS, and UV (36). Set2 cooperates with the H3K9 methyltransferase Clr4 to regulate the expression of Mik1, a CDK inhibitory kinase. The degree of H3K36 methylation (H3K36me) (di- or tri-) and type of modification (acetylation or methylation) will influence the choice of DSB repair pathway that is activated (37–39). However, how Set2 safeguards cell viability in the presence of MMS is unclear.

Here, we interrogated the molecular mechanisms underlying the Set2-dependent response to MMS. We show that Set2 is epistatic with DNA damage checkpoint factors to enforce the timely recruitment of NER and HR factors in response to MMS. Our findings thus point to a model in which Set2 and the methylation of H3K36 control the sensing and repair of alkylating damage in fission yeast.

MATERIALS AND METHODS

Yeast strains and media

The *S. pombe* strains used in this study are listed in Supplementary Table S1. Standard procedures for manipulating *S. pombe* strains were followed (40,41). Complete YEA (3% glucose, 0.5% yeast extract, 75 mg/l adenine) was used as the culture media for yeast cells. Double mutant strains were generated through crossing of parental strains, followed by separation of meiotic progenies by tetrad dissection analysis using an MSM manipulator (Singer Instruments, Watchet, Somerset, UK). Appropriate gene disruption was checked with PCR, as previously described (42,43).

Spotting analysis

Spotting analyses were carried out as previously described (43,44). Briefly, asynchronously growing cells were concentrated to 10^7 cells/ml, and then titrated with a 5-fold or 10-fold serial dilution. Cells were then spotted on YEA plates with or without MMS. Plates were incubated at 30°C for 3 days before analysis.

Construction of Set2 domain deletion (SDD) strains

The secondary structure of Set2 was predicted using online PSIPRED Protein Sequence Analysis Workbench (http://bioinf.cs.ucl.ac.uk/psipred/) to determine a truncation site in an unstructured loop (not in a defined secondary structure such as a α helix or β sheet; 45) (Supplementary Figure S1). Eight SDD strains were generated using overlapping PCR-based procedures (Supplementary Figure S2). Each of the truncated *set2* mutants was tagged with 3× hemagglutinin (HA) to determine protein levels. The domains removed were: N-terminus (SDD1), pre-SET (SDD2), SET (SDD3), post-SET (SDD4), linker (SDD5), domain of unknown function (DUF) (SDD6), Set2-Rpb1 interacting (SRI) (SDD7) and C-terminus (SDD8).

Immunoblotting

Asynchronous cells growing at 30°C were incubated with 0.01% MMS. Cells were collected at different time points up to 4 h. Total protein was extracted using trichloroacetic acid (46,47), separated on polyacrylamide gels, and transferred to Hybond ECL nitrocellulose membranes (GE Healthcare, Little Chalfont, UK). Membranes were incubated with primary antibodies for 1 h at room temperature, washed, and then incubated with secondary antibodies for 1 h. Chemiluminescence was performed with Amersham ECL Prime (GE Healthcare) and chemiluminescence detection and band intensity quantification were achieved using an ImageQuant LAS 4000 imager (GE Healthcare). The primary antibodies used were: α-HA (12CA5, Roche Applied Science; Basel, Switzerland), α-GFP (1181446001, Roche Applied Science), α-H3K36me2 (CS-127-100, Diagenode), α-H3K36me3 (ab9050, Abcam) and α-Cdc2 (sc-53, Santa Cruz Biotechnology; Dallas, TX, USA). The secondary antibodies, goat-anti-mouse IgG-HRP (sc-2005) and goat-anti-rabbit IgG-HRP (sc-2004), were from Santa Cruz Biotechnology.

Fluorescence microscopy

Cells expressing GFP-tagged Rhp54 or Rhp23 were fixed with methanol, as previously described (47). GFP fluorescence was observed using a Nikon Eclipse Ti-E fluorescence microscope (Nikon; Tokyo, Japan), and Z-stack images were obtained. Cells were counterstained with 4′,6-diamidino-2-phenylindole (DAPI) (Life Technologies; Carlsbad, CA, USA). Rhp23-GFP nuclear staining and Rhp54-GFP foci number were quantified using Nikon NIS-Element software. Rhp54-GFP foci were determined as outlined in Supplementary Figure S3.

Chromatin immunoprecipitation (ChIP)

Cells were treated with 3% formaldehyde and fixed with 10 mM dimethyl adipimidate (DMA) (Sigma-Aldrich; St Louis, MO, USA) for 45 min. ChIP assay was performed as previously described (47). Bands from competitive PCR between *brc1*$^+$ locus and the control *act1*$^+$ were quantified using ImageQuant TL software (GE Healthcare).

Determination of protein turnover for Rhp23

Log-phase cells were combined with varying combinations of 0.01% MMS, 100 μg/ml cycloheximide (CHX), and 50 μM of MG132 (all from Sigma-Aldrich) and incubated for 2 h at 30°C. Cells were harvested for western blotting. DMSO was used as solvent control for MG132.

Reverse Transcription-PCR

Total RNA from WT and *Δset2* cells was extracted using Trizol reagent (Life Technologies), then treated with DNase I (Thermo Fisher Scientific), as previously described (47). cDNA was prepared using the One-Step RT-PCR kit (Qiagen; Venlo, Netherlands) and primers targeting the genes of interest. The reverse-transcribed cDNA was further amplified using PCR.

Viability assay

Cell cultures were treated with varying concentration of MMS (0%, 0.005%, 0.01%, 0.02% and 0.03%) and incubated at 30°C for 2 h. Cultures were plated onto YEA plates in equal amounts, and the number of colonies on YEA plates were quantified. The % survival was calculated by comparing the number of colonies obtained from the MMS-treated cells normalized to the untreated cells.

RESULTS

Response to MMS is dependent on the SET domain of Set2 and H3K36

Previous studies have shown that *Δset2* cells are hypersensitive to various DNA damaging agents, including bleomycin, phleomycin, HU and MMS (36,37,48). Although the molecular mechanisms underlying hypersensitivity to most of these agents in *Δset2* cells have been elucidated, MMS susceptibility remains unclarified. We therefore sought to investigate the DDR pathways involved in cellular response to MMS in *Δset2*.

First, to check whether MMS sensitivity (Figure 1A) was dependent on methylation of H3K36 by Set2, we created a mutant strain expressing a lysine-36 to arginine mutant (K36R) protein from the only remaining genomic copy of the histone H3 gene *hht2*$^+$ (Supplementary Table S1). The *H3K36R* mutant was hypersensitive to MMS compared with *Δset2* cells, suggesting that H3K36 methylation (H3K36me) is required for enacting the response to DNA alkylating damage (Figure 1B).

We then constructed eight truncation mutants (SDD1–8), each lacking one of the modular domains within the Set2 protein, referred to as 'Set2 domain deletion (SDD) mutants' (Figure 1C). Western blot analysis of the HA-tagged SDD mutants showed that truncation of individual domains did not affect the overall stability of the Set2 protein (Figure 1D). Truncation of the SET and surrounding domains (SDD1–5) abolished the H3K36 methyltransferase activity of Set2 (Figure 1E), whereas truncation of SRI and surrounding domains (SDD6–7) still resulted in considerable H3K36me2 levels but much reduced H3K36me3 levels. The SDD8 mutant, however, resembled WT cells, with no observable H3K36me2 but clear H3K36me3 expression.

We next serially diluted log-phase growing WT and SDD cells on media incorporated with 0.02% MMS (Figure 1F) to ascertain the role of each domain on MMS hypersensitivity. SDD1–7 mutants exhibited a similar level of MMS hypersensitivity as *Δset2* cells (mutant cells devoid of Set2 function). As expected, growth of SDD8 was indistinguishable from WT cells. Taken together, these results indicate that MMS sensitivity depends on H3K36 and, particularly, on the SET domain of Set2.

Set2 is epistatic with DNA damage checkpoint factors and regulates the checkpoint effector, Chk1

Next, we performed epistasis analyses to explore the role of Set2 in DNA damage sensing. We generated double mutant strains that harbored a deletion of *set2* and a deletion of the gene for one of the following: DNA damage sensor

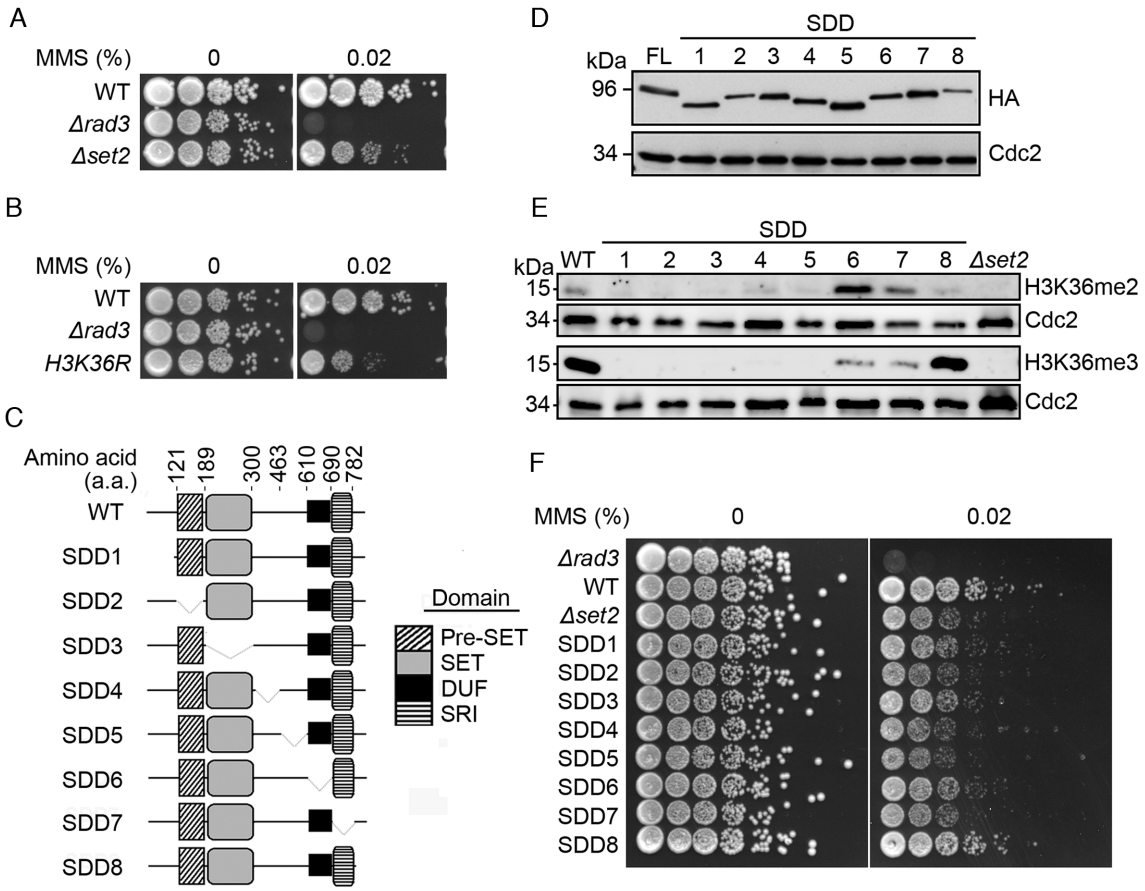

Figure 1. H3K36 and SET domain of Set2 are required for tolerance to methyl methanesulfonate (MMS) in fission yeast. (**A**) Set2 mutant (*Δset2*) and (**B**) *H3K36R* mutant were tested on YEA plates incorporated with 0.02% MMS. *Δrad3* serves as a control. WT: wild-type. (**C**) Schematic representation of Set2 domain deletion (SDD) mutants with progressive truncation of the modular domains within the protein. Amino acid numbers (top) indicate the position of the modular domains. DUF: Domain of unknown function, SRI: Set2-Rpb1 Interacting. (**D**) Protein expression of 3 × HA-tagged SDDs and the corresponding loading control, Cdc2. Results shown are representative of two experiments. FL, full length of Set2. (**E**) H3K36me2 and H3K36me3 levels in the SDD strains. (**F**) SDD strains are sensitive to MMS. SDD1–8 strains were 5-fold serially diluted and spotted on plates containing 0.02% MMS. Plates were incubated for 3 days at 30°C.

Rad3 (*S. pombe* homolog of ATR), Tel1 (ATM homolog) or PCNA-like sliding clamp (Rad9, Rad1 and Hus1); replication checkpoint protein Cds1; MRN component Rad32; and DNA damage checkpoint proteins, Crb2 and Chk1.

Rad3 acts as the sensor kinase to relay the DNA damage signal for the activation of cell cycle checkpoint and damage repair pathways, and *Δrad3* cells were unable to activate the checkpoint and halt the progression of the cell cycle in the presence of MMS, causing cell death (49). In contrast, the *tel1* null mutant was less sensitive to MMS, presumably because Tel1 is more important in maintaining telomere integrity in fission yeast than having a role in DDR (50). Interestingly, deletion of both *set2* and *rad3* marginally suppressed the growth defect of *Δrad3* at 0.005% MMS, indicating that the absence of *set2* can partially bypasses the MMS susceptibility associated with the loss of *rad3*. Comparatively, the *Δtel1Δset2* double mutant showed no increased sensitivity to MMS, indicating that Tel1 and Set2 act in the same functional group to confer tolerance to MMS (Figure 2A).

Binding of the Rad9-Rad1-Hus1 heterotrimeric complex to damaged chromatin can facilitate the Rad3-dependent phosphorylation and activation of the downstream checkpoint kinases Chk1 (for DNA damage) and Cds1 (for replication block) (13,51,52). As expected, *Δrad1*, *Δrad9* and *Δhus1* were all hypersensitive to a low concentration of MMS (0.002%) (Figure 2B) but the further deletion of *set2* did not enhance the growth defect. The consistency observed among the different units of the complex suggests that defects in the *set2* mutant may involve attenuation of the DNA damage checkpoint when exposed to MMS (Figure 2B).

MMS treatment activates the G2/M checkpoint to delay entry into mitosis. This can involve the activation of the intra-S checkpoint when the replication fork encounters alkylated bases (53). We found that the *cds1* mutant showed only slight sensitivity even to higher concentrations (0.02%) of MMS as compared with the *Δset2* mutant (Figure 2C). The *Δcds1Δset2* double mutant was more resistant to MMS, which may be connected to a more efficient formation of HR repair foci (see below). On the contrary, the *H3K36R* mutant—which showed a stronger MMS hypersensitivity compared to *Δset2* (Figure 1A, B)—was sup-

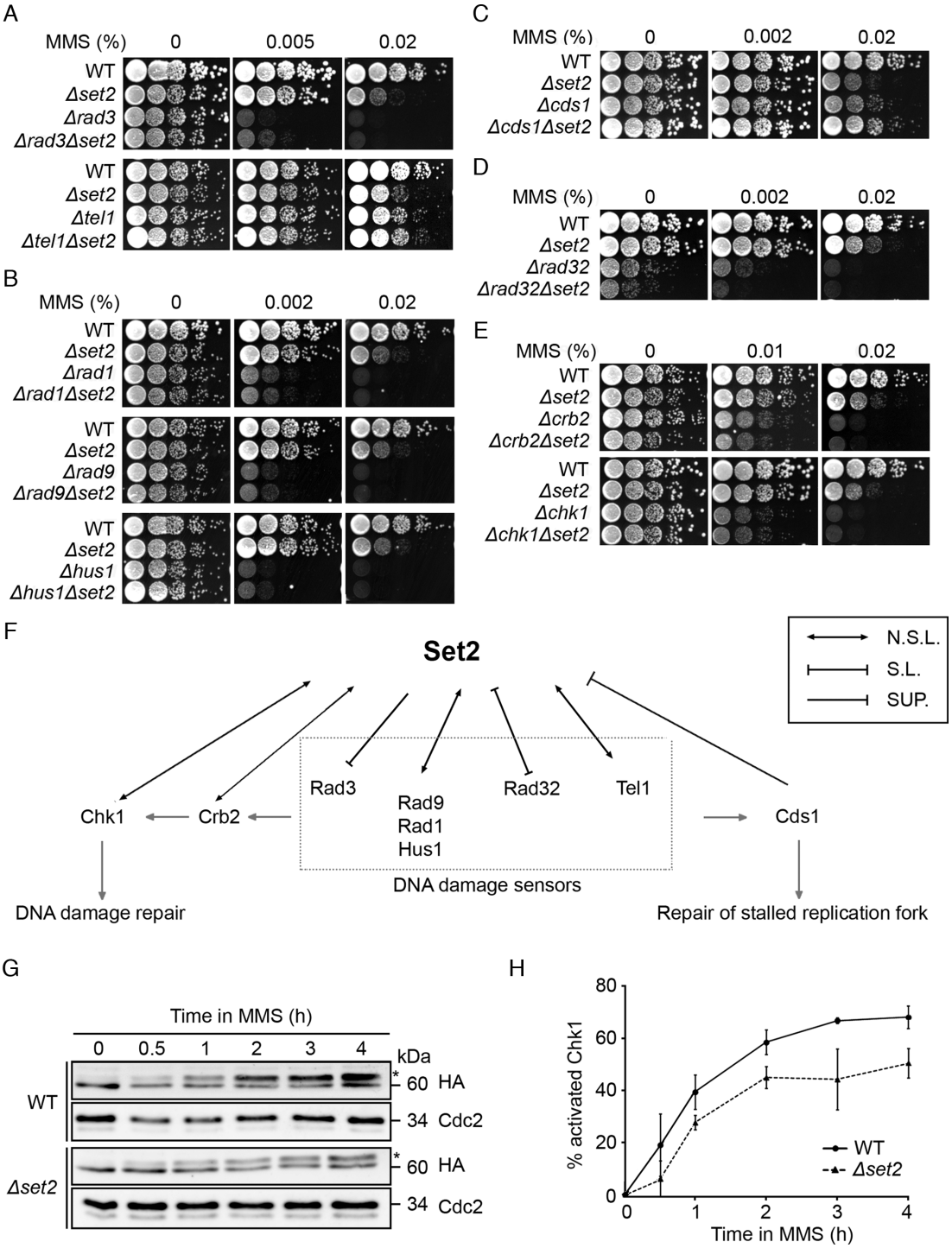

Figure 2. Genetic interaction between Set2 and DNA damage response factors. Interaction of *Δset2* with the following DNA damage pathway mutants in the presence of varying concentrations of methyl methanesulfonate (MMS): (**A**) *Δrad3* and *Δtel1*, (**B**) *Δrad1*, *Δrad9* and *Δhus1*, (**C**) *Δcds1*, (**D**) *Δrad32*, (**E**) *Δcrb2* and *Δchk1*. (**F**) Schematic diagram of a simplified DNA damage response network to illustrate the genetic interactions of Set2 with the tested DNA damage pathway factors. Arrows are: N.S.L, non-synthetic lethal. S.L., synthetic lethal. SUP., suppression. (**G**) Protein expression of 3 × HA-tagged Chk1 in WT and *Δset2* cells after treatment with 0.01% MMS over 4 h at 30°C. Results shown are representative of three experiments. (**H**) The percentage of activated Chk1 was calculated by quantifying the intensity of the upper band (*) of 3 × HA-tagged Chk1 over the sum of the upper and lower bands in (G). Bars and error bars represent the mean ± S.D., respectively.

pressed by *Δcds1* relative to *Δset2*; albeit to a lower extent (Supplementary Figure S4A).

Unlike its mammalian counterpart, the fission yeast MRN complex (Rad32–Rad50–Nbs1) is not required for the G2 DNA damage checkpoint or general damage recognition but is required for delaying the S-phase checkpoint and activating recombination to repair the damaged DNA strand (54). In the absence of MMS, *Δrad32* cell growth was slower than that of WT cells, as Rad32 is required to repair spontaneous fork collapses during the normal cell cycle (Figure 2D) (55). Comparing the relative growth differences between *Δrad32* and WT cells on plates with or without drug, we found that *Δrad32* cells were sensitive to MMS at 0.002%, and this was exacerbated in double mutant cells (*Δrad32Δset2*), suggesting that Set2 may act in parallel with the S-phase checkpoint to confer resistance to MMS.

Upon DNA damage, Chk1 phosphorylation by Rad3 results in cell cycle arrest. This proceeds through the phosphorylation of downstream cell cycle transition factors, Wee1 and Cdc25 (56,57). Both *Δcrb2* and *Δchk1* mutants showed MMS hypersensitivity but this was not increased by the concurrent deletion of *set2* (Figure 2E).

Taken together, Set2 functions in a similar epistasis group as components of the DNA damage response arm, including DNA damage sensors and checkpoint proteins, but is synergistic to the MRN component, likely to protect cells against alkylating damage associated with MMS treatment. Unexpectedly, instead of a synergistic relationship, Set2 shows an indirect relationship with the DNA replication checkpoint in response to MMS (Figure 2F).

Set2 is required for prompt Chk1 activation in response to MMS

The non-synthetic lethal phenotype of *Δcrb2Δset2* and *Δchk1Δset2* raised a possibility that Set2 may regulate DNA damage checkpoint proteins to confer tolerance to MMS (Figure 2E). To determine whether the sensitivity of *Δset2* may be connected to a checkpoint activation defect, asynchronous WT and *Δset2* cells bearing 3 × HA-tagged Chk1 were exposed to 0.01% MMS and monitored for changes in the activation of Chk1 (slower migrating band corresponds to phosphorylated Chk1) (58). Whole cell lysates were collected hourly after the addition of MMS until 4 h, and prepared for immunoblotting (Figure 2G). In WT cells, there was a high level of activated Chk1 (upper band) after 0.5 h of MMS exposure, and by 4 h, 69% of Chk1 was activated (Figure 2H). Surprisingly, in *Δset2* cells, although the timing of Chk1 activation was the same, the levels of phosphorylation were considerably lower, with only 50% of Chk1 activated after 4 h of MMS treatment (Figure 2H). These results suggest that Set2 (directly or indirectly) regulates Chk1 activation.

Set2 acts in the NER epistasis group to respond to MMS-induced alkylating damage

In fission yeast, MMS alkylating damage is repaired by both BER and NER pathways (26,59). If the lesion is not repaired, it will cause the replication fork to stall, which, in turn, leads to fork collapse and the formation of DSBs. These DSBs are instead repaired by NHEJ or HR, and intermediates formed during BER are also repaired by HR (60).

To investigate whether Set2 participates in the initial repair pathway for MMS damage by BER, *set2* was deleted in *apn2* and *nth1* mutants: Apn2 is the AP endonuclease that removes repair intermediates after the excision of alkylate-damaged bases by DNA glycosylases, whereas Nth1 is a DNA glycosylase that functions upstream of Apn2 to remove the oxidized bases from MMS-mediated damage (24). As expected, *Δapn2* and *Δnth1* were sensitive to 0.01% MMS (Figure 3A), and deletion of *set2* further sensitized the cells to a lower MMS concentration (0.005%). We then measured the viability of single and double mutants of *Δset2* and *Δapn2*, and found that the double mutant significantly aggravated the hypersensitivity of each of the single mutants to alkylating damage (Figure 3C, left). These results suggest that both Set2 and BER factors function in parallel to maintain cell viability in response to MMS. Consistent with the higher intolerance of *H3K36R* to MMS, *Δapn2H3K36R* showed over 100-fold hypersensitivity to 0.005% MMS (Supplementary Figure S4B) compared with the minimal reduction in growth noted for *Δapn2Δset2* cells in the same concentration of MMS (Figure 3A).

In fission yeast, BER acts synergistically with NER, as shown by an increase in MMS sensitivity when factors from both pathways are concurrently mutated (26,61). As Set2 shows synergistic interaction with BER factors, it is likely that Set2 may have a close interaction with NER or possibly work in a similar repair pathway to NER. To confirm this hypothesis, *set2* was deleted in the following NER mutants: *Δrhp23* (human hHR23A and hHR23B for damage recognition), *Δrad13* (human XPG ortholog with endonuclease function) (62,63), *Δrhp7*, and *Δrhp26* (human CSB) (Figure 3B). Rad13 and Rhp23 function in both GGR and TCR pathways but Rhp7 functions in the GGR pathway and Rhp26 in the TCR arm (27,64). Interestingly, none of the *Δrhp26Δset2, Δrad13Δset2* and *Δrhp23Δset2* double mutants showed higher MMS hypersensitivity over the respective single mutants. This was further confirmed by the viability of the *Δrhp23Δset2* cells, where the concurrent loss of both proteins led to similar intolerance towards MMS relative to the single mutants (Figure 3C, right). On the other hand, *Δset2* MMS hypersensitivity was partially suppressed by *Δrhp7* mutation (Figure 3B). These results suggest that Set2 participates in the same group as NER factors, possibly in the TCR pathway, to protect against MMS.

Set2 regulates the nuclear enrichment of NER factors in MMS

Lesion binding and recognition by the Rhp23-Rhp41 complex is a critical step in the initiation of alkylation-mediated DNA damage repair (65). Since Set2 is epistatic to NER pathway factors in regulating MMS resistance, we tested whether Set2 may regulate the recruitment of the Rhp23–Rhp41 complex. For this purpose, we epitope-tagged Rhp23 with GFP expressed from the original chromosomal locus and studied its cellular localization (Fig-

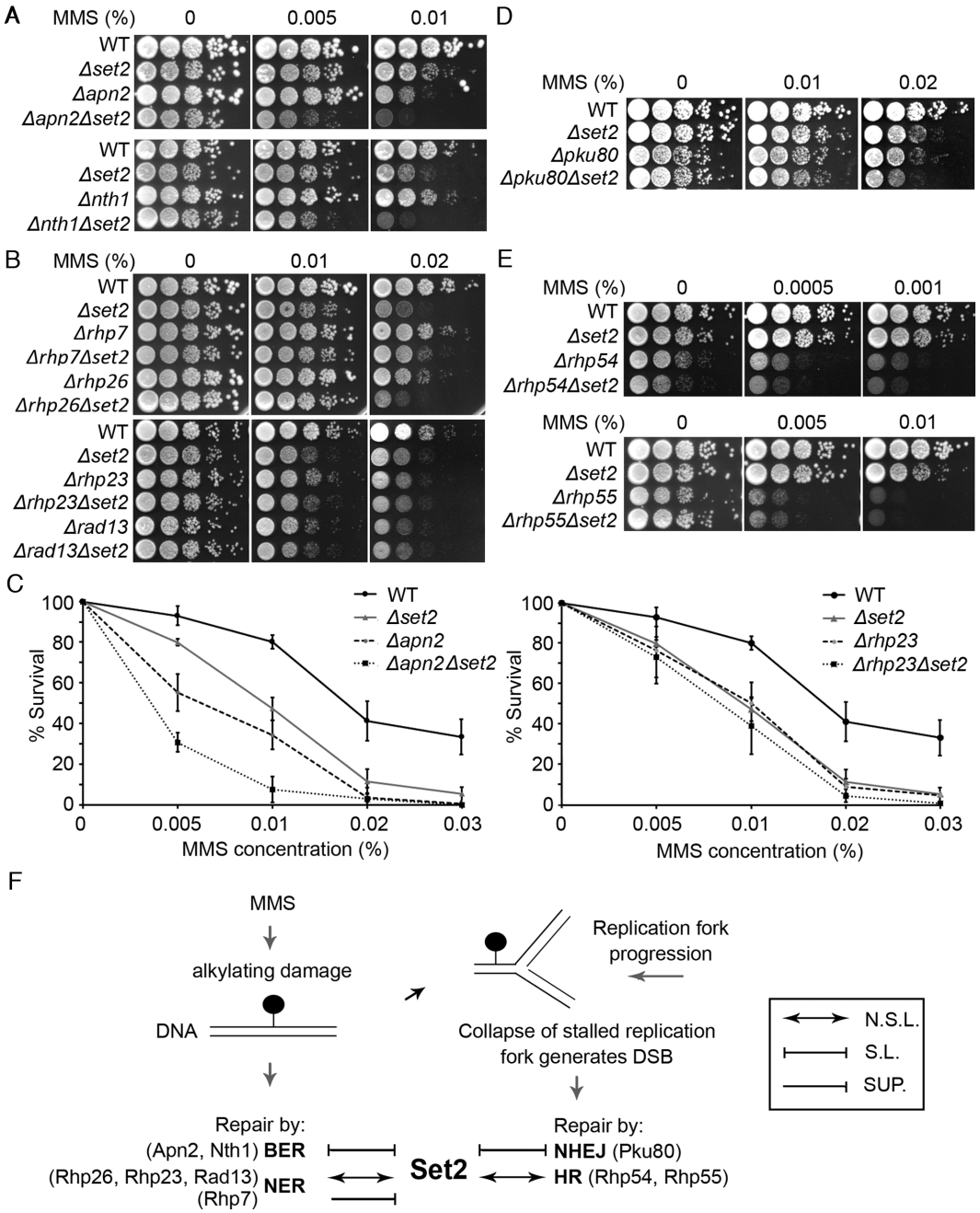

Figure 3. Genetic interaction of Set2 with representative factors from various DNA damage repair pathways. Sensitivity of WT and *Δset2* in methyl methanesulfonate (MMS) was tested together with single and double mutants for pathway components of (**A**) BER (*Δapn2, Δnth1* and the double mutants *Δapn2Δset2* and *Δnth1Δset2*), (**B**) NER (*Δrhp7, Δrhp26, Δrhp23, Δrad13, Δrhp7Δset2, Δrhp26Δset2, Δrhp23Δset2* and *Δrad13Δset2*), (**D**) NHEJ (*Δpku80* and *Δpku80Δset2*), and (**E**) HR (*Δrhp54, Δrhp55, Δrhp54Δset2* and *Δrhp55Δset2*). (**C**) Viability assay for WT, *Δset2, Δapn2, Δapn2Δset2, Δrhp23* and *Δrhp23Δset2* in different concentration of MMS for 2 h at 30°C. Bars and error bars represent the mean ± S.D., respectively. (**F**) Schematic representation of the various DNA damage repair mechanisms for repairing alkylating damages induced by MMS, and a summary of the genetic interactions of these factors with Set2. Abbreviations: *DSB*, double-stranded breaks; *BER*, base excision repair; *NER*, nucleotide excision repair; *HR*, homologous recombination repair; *NHEJ*, non-homologous end joining repair; *N.S.L.*, non-synthetic lethal; *S.L.*, synthetic lethal. *SUP.*, suppression.

ure 4A and Supplementary Figure S5). In WT cells, there was a time-dependent increase in the nuclear localization of Rhp23-GFP after MMS treatment (Figure 4B and D). Interestingly, the MMS-dependent nuclear enrichment of Rhp23 was significantly lower in both the *Δset2* and *H3K36R* mutants as compared with WT cells (Figure 4A, B and D), with Rhp23 protein levels relatively similar across the different strains (Figure 4C and E). Together, these results suggest that Set2 exerts its effect on NER by regulating Rhp23 nuclear localization after alkylation damage, and suggest that Set2 might act further upstream in the NER pathway.

We next considered the possibility that Set2 coordinates proteasome-dependent degradation of Rhp23. The budding yeast counterpart of Rhp23, Rad23, is reported to be ubiquitinated; however, the ubiquitin-associating domain nested in the C-terminus shields the ubiquitination signal from proteasomal degradation (66). If this regulation also works in fission yeast, then the decrease in Rhp23 signals may be linked to an increased rate of protein turnover in the absence of *set2*. We thus determined the protein level of Rhp23 in WT and *Δset2* cells with or without MMS in the presence of 50 μM MG132, a proteasome inhibitor, and 100 μg/ml cycloheximide (CHX), a protein synthesis inhibitor (67,68). We found similar levels of Rhp23 in the WT and *Δset2* cells in the presence or absence of MMS, MG132, and CHX, indicating that proteasomal degradation is not the mechanism underlying the localization of Rhp23 by Set2 (Supplementary Figure S6).

Next, we considered whether Set2 confers chromatin recruitment of Rhp23 to mediate alkylation-mediated damage repair. We searched previously published, genome-wide gene expression datasets generated in response to various stresses arising from exposure to oxidative damage, heat, cadmium (a heavy metal cation), and MMS (69) to determine which gene sequences we could use for ChIP. We first selected genes that showed altered expression in MMS, as alkylation-type damage imposed onto the gene loci should impede RNAPII and cause a decrease in transcription. However, our ChIP results did not identify any Rhp23 recruitment (data not shown). We then searched for genes that were induced by other stressors but found gene downregulation only following insult with MMS. Among these genes, we identified *brc1*$^+$, which encodes a BRCT domain protein required for DNA damage repair (70,71). Through ChIP, we found Rhp23 to be preferentially recruited to the chromatin on this gene locus at 15 to 30 min after MMS exposure relative to the *act1* locus (Figure 4F). However, in the absence of *set2*, Rhp23 localization to the *brc1* locus was reduced by 28% at 15 min and 40% at 30 min after drug treatment (Figure 4G). Interestingly, although *brc1*$^+$ expression showed a minor decreasing trend (only statistically significant at 30 min) over the course of 0–60 min MMS treatment in WT cells, *brc1*$^+$ transcription was significantly downregulated (16% at both 15 and 30 min) in the absence of *set2* (Supplementary Figure S7A). Overall, these results suggest that Rhp23 is recruited to chromatin at specific gene regions for an effective response toward MMS insult (Supplementary Figure S7B).

Set2 regulates the dynamicity of Rhp54 in DNA repair foci formation after MMS treatment

As mentioned above, prolonged damage by MMS results in fork collapse and DSBs, which are repaired by NHEJ or the error-free HR. In yeast, HR is the preferred method of repair during S- and G2-phase defects, whereas NHEJ is limited to defects within the G1 phase (72). Because H3K36me is found at DSBs, it may participate in the DSB repair pathway (38). To determine which pathway is involved, we carried out genetic interaction studies between Set2 and the NHEJ factor Pku80, and HR factors, Rhp54 and Rhp55. Pku80 forms a heterodimer with Pku70, and promotes NHEJ by binding to DSB ends and recruiting other NHEJ factors (73). We found that MMS sensitivity of *Δpku80* was comparable to that of *Δset2* but the *Δpku80Δset2* double mutant showed increased sensitivity, suggesting that Set2 functions in parallel with NHEJ in DSB repair (Figure 3D). However, for single mutants of HR factors, growth in the absence of the drug was slower than that of WT cells, and the mutants were hypersensitive to low MMS concentrations (0.0005% and 0.005%; Figure 3E). There was no additional MMS sensitivity in the double mutant, suggesting a close relationship between HR factors and Set2 (Figure 3F).

To decipher the molecular mechanism of how Set2 functions in HR-dependent DSB repair, Rhp54 was tagged with GFP at the C-terminus in both WT and *Δset2* cells. Using microscopy, we show that in WT cells, Rhp54-GFP formed foci after the addition of MMS (Figure 5A), with an increasing number of cells with GFP-positive foci over time (Figure 5B). Yet, in *Δset2* cultures, there were fewer cells contained Rhp54-GFP foci after MMS treatment (2 to 4 h) as compared with WT cultures (Figure 5A and B). The protein level of Rhp54 increased after the addition of MMS, consistent with previous reports (58,74). The reduced number of Rhp54-GFP foci formed in *Δset2* was not due to a difference in protein expression (Figure 5C). These data suggest that Set2 facilitates the timely recruitment of HR machinery in response to MMS-induced damage. Further, we find that the effect of Set2 on Rhp54 foci formation is dependent on H3K36me, as the *H3K36R* mutant shows similar defects in Rhp54-GFP foci formation during MMS treatment, and the expression of Rhp54 remains unaffected by the *H3K36R* mutation (Figure 5D, E and Supplementary Figure S8).

Deletion of *cds1* in the *Δset2* background caused a 25% increase in the number of cells exhibiting more than four Rhp54 foci as compared to the *Δset2* single-null mutant, suggesting that Cds1 may negatively regulate foci formation of Rhp54 in *Δset2* cells (Supplementary Figure S9). Chk1 phosphorylation did not significantly differ between *Δcds1Δset2* and *Δset2* cells, suggesting that the partial restoration of Rhp54 localization is independent of the DNA damage checkpoint (Supplementary Figure S10). Taken together, these results indicate that Set2 confers MMS tolerance via the effective activation of NER and HR mechanisms.

DISCUSSION

Set2 was recently reported to play an essential role in DNA damage, particularly in the repair of DSBs (36,37,48). Here,

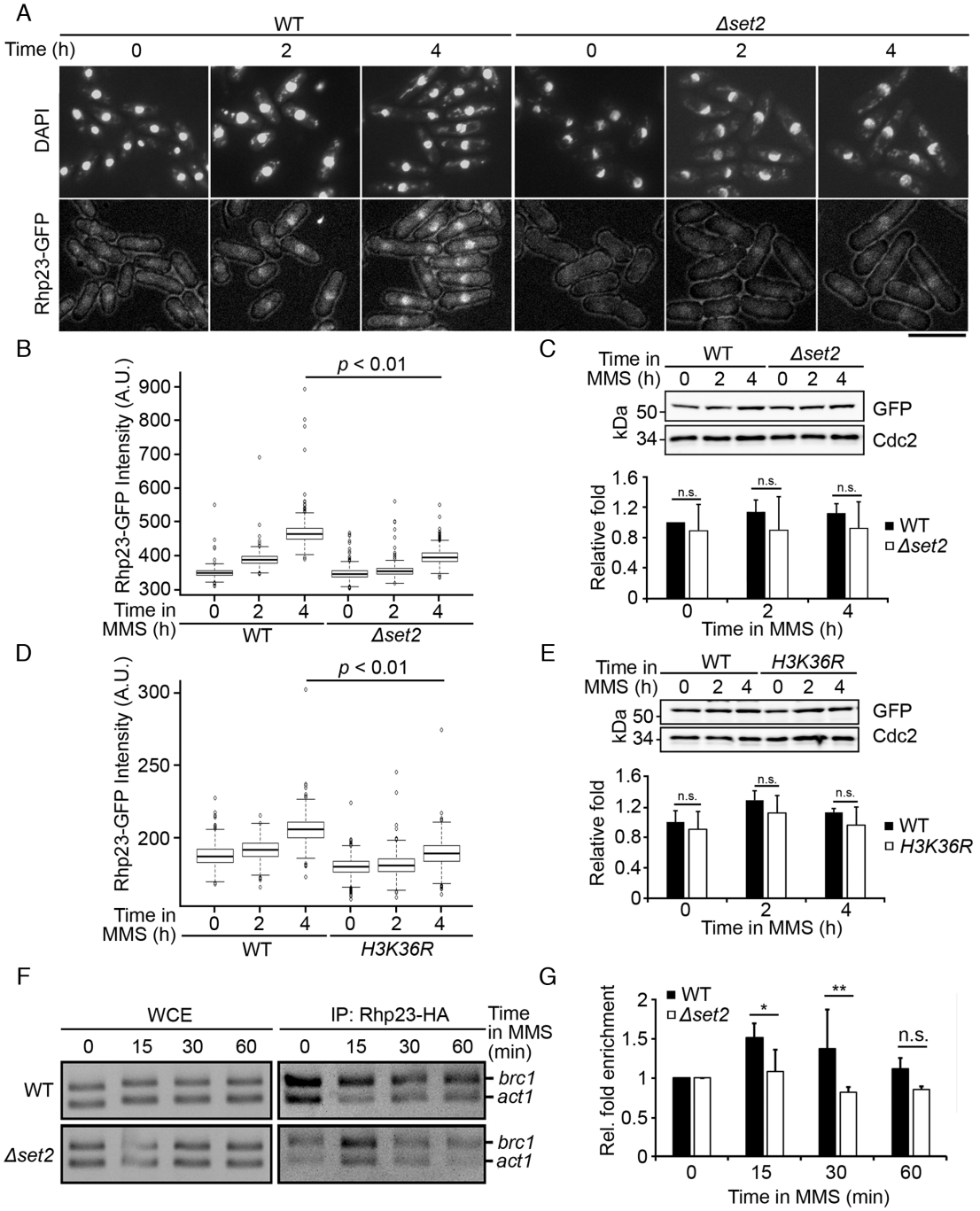

Figure 4. Set2-dependent nuclear localization of Rhp23 during methyl methanesulfonate (MMS) treatment. (**A**) Microscopic observation of GFP-tagged Rhp23 (Rhp23-GFP) and nuclear staining (DAPI) in WT and *Δset2* cells after treatment with 0.01% MMS for the indicated times. Scale bar: 10 μm. (**B** and **D**): Box-and-whisker plot showing the GFP intensity of nuclear-localized Rhp23 in WT and *Δset2* (B) and *H3K36R* (D) cells after treatment with 0.01% MMS. $n = 700$. The box spans from 25th to 75th percentile, with the black line indicating the median, whisker extending to 10 and 90 percentile range. Statistical comparison of WT and *Δset2* at 4 h was performed using F-test, followed by Welch *t*-test. Statistical significance between WT and *Δset2*, and between WT and *H3K36R* at 4 h of $P < 0.01$ and $P < 0.01$ were respectively detected. Overall fluorescence difference between (B) and (D) may be due to experimental variation and/or that in genetic background as strains in (D) contained *Δhht1* and *Δhht3* (Supplementary Table S1). (**C** and **E**): Protein expression of Rhp23-GFP in WT and *Δset2* (C) and *H3K36R* (E) after treatment with 0.01% MMS (top). Graph of the mean relative band intensity quantification from three experiments (bottom). Black, WT; white, *Δset2* or *H3K36R*. (**F**) ChIP assay of Rhp23-HA in WT and *Δset2* cells treated with 0.01% MMS for 0, 15, 30 and 60 min. ChIP was analyzed using competitive PCR with primers specific for *brc1*$^+$, with *act1*$^+$ as a control. (**G**) Graph of the relative fold enrichment was calculated by comparing the ratio of *brc1*$^+$/*act1*$^+$ between the IP samples and whole-cell extracts (WCE) and normalized to the time point of '0' (= 1) for each strain. Bars and errors bars represent mean ± S.D., respectively, from three independent experiments. *n.s.*, not significant; *$P < 0.05$; **$P < 0.01$.

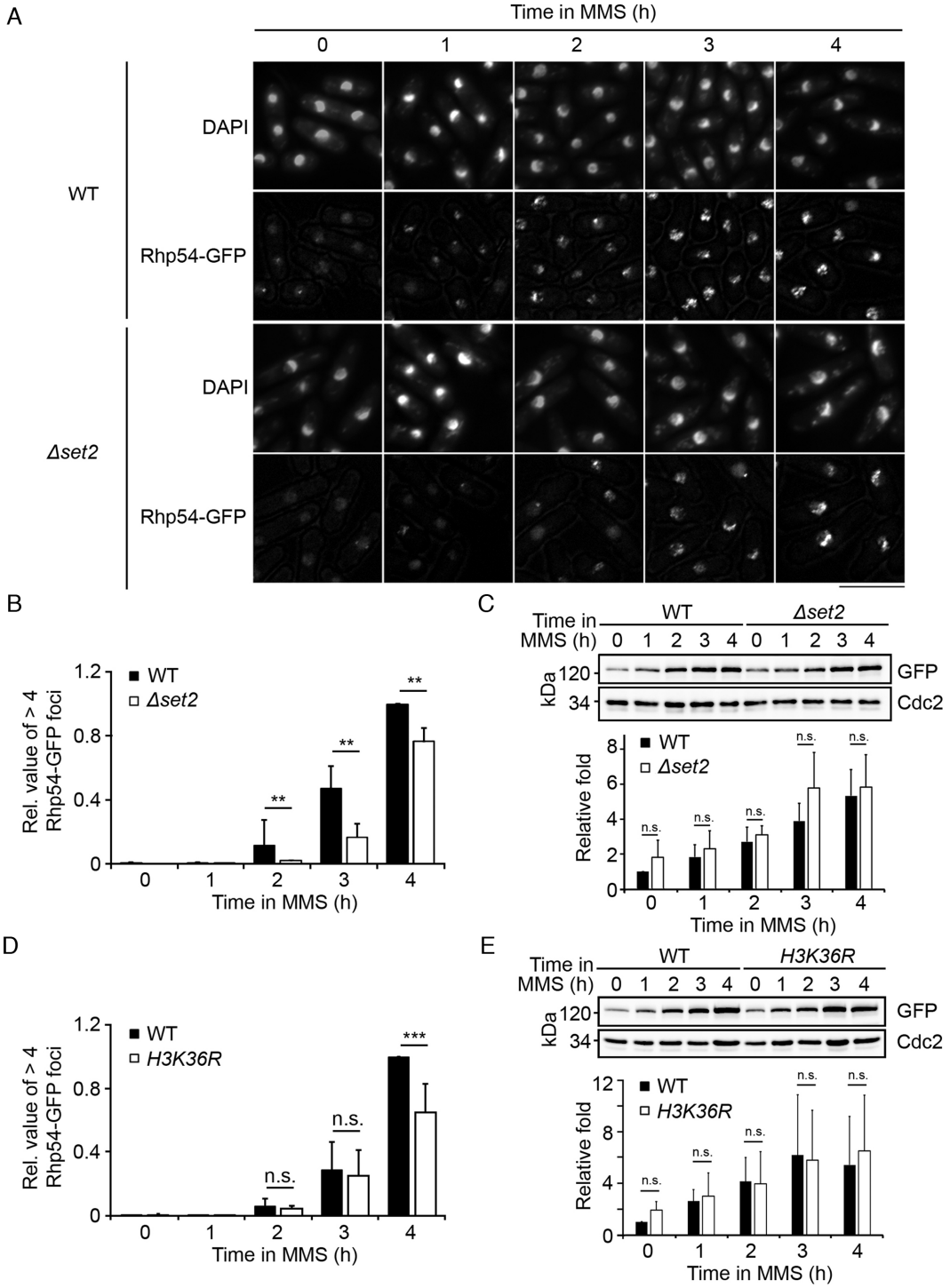

Figure 5. Set2 is required for the timely formation of Rhp54 DNA damage repair foci. (**A**) Microscopic observation of GFP-tagged Rhp54 (Rhp54-GFP) foci formation and nuclear staining (DAPI) after the addition of 0.01% methyl methanesulfonate (MMS) at 30°C for 4 h in WT and *Δset2* cells. Scale bar: 10 μm. (**B**) Relative value of *Δset2* cells with >4 Rhp54-GFP foci in (A) was determined relative to WT at 4 h. $n = 700$. $^{**}P < 0.01$. Fisher's exact test. (**C**) Protein expression of Rhp54-GFP in WT and *Δset2* cells after treatment with 0.01% MMS for 4 h. Graph shows quantification of the relative band intensity (bottom). Black, WT; white, *Δset2*. Results shown are an average of three experiments. Bars and error bars represent mean ± S.D., respectively. *n.s.*, not significant, two-tailed *t* test. (**D**) Relative value of *H3K36R* cells with >4 Rhp54-GFP foci was determined relative to WT at 4 h. $n = 700$. *n.s.*, not significant; $^{***}P < 0.001$. Fisher's exact test. (**E**) Protein expression of Rhp54-GFP in WT and *H3K36R* cells after treatment with 0.01% MMS for 4 h. Graph shows quantification of the relative band intensity (bottom). Black, WT; white, *H3K36R*. Bars and errors bars represent mean ± S.D., respectively, from three biological repeats. *n.s.*, not significant, two-tailed *t* test.

we investigated the mechanistic regulation of tolerance by Set2 against alkylation damage in fission yeast cells. We demonstrate the importance of H3K36me and the SET domain, which mediates the methyltransferase activity of Set2, in conferring resistance against MMS. Through genetic interaction studies, we show that Set2 cooperates with factors of the DDR, regulates the activation of Chk1, and facilitates Rhp54-GFP foci formation in response to MMS exposure. We also show that Set2 affects the cell's response to MMS by acting in the NER pathway and regulating the nuclear localization of Rhp23. Taken together, these results indicate a novel role of Set2/H3K36me in DDR in facilitating checkpoint activation, repairing alkylating damage through NER, and recruiting HR repair proteins, possibly to sites of DSBs.

Genetic interaction study of Set2 and DDR factors

We show that Set2 is in the same epistasis group as the DNA damage checkpoint. In fission yeast, the MRN complex recruits DNA end-processing factors Tel1 and Ctp1 to sites of DSBs to facilitate end resection and HR (14). Tel1 activates Chk1 but this only occurs when both Ctp1 and Rad3 are deleted. A previous study in mammalian cells has shown that H3K36me2 is enriched at DSBs, facilitating the recruitment of NBS1 and Ku70 for break repair by NHEJ (38). Indeed, H3K36me2 directly recruits NBS1 to such locations (75). However, our results do not favor the involvement of H3K36me in the direct recruitment of the MRN complex or in the activation of Chk1 by Tel1 for the following reasons: First, *Δset2* was not synthetic lethal with *Δtel1*. Second, in fission yeast, the MRN complex functions at the S-phase checkpoint rather than in response to general damage recognition or DNA damage checkpoints (54). Furthermore, double mutants of *Δset2* and the 9–1–1 complex were not synthetic lethal, suggesting that Set2 likely functions in DNA damage checkpoints rather than in DNA replication checkpoints. Third, a synthetic lethal effect was observed in *Δrad32Δset2* cells, suggesting that Set2 is not in the same epistasis group as the MRN–Tel1–Chk1 pathway. This negative genetic interaction indicates that Set2 functions in parallel or acts as a compensatory mechanism in mediating resistance to MMS when the MRN–Tel1–Chk1 pathway is defective.

Set2 acts in the NER pathway against MMS damage

Double mutants of Set2 with NER factors Rhp26, Rhp23 and Rad13 showed no cumulative effect, suggesting that these proteins may work in a similar functional group. Rhp7 and Rhp26 function in the GGR and TCR subpathways of NER, respectively. These sub-pathways are differentiated by the initial lesion recognition steps: GGR factors recognize transcription inactive regions in the genome, whereas TCR factors sense DNA lesions during transcription elongation by RNAPII (29,76). Since Set2 is a transcription elongation factor that associates with RNAPII, it is not surprising to find its involvement in TCR. Hence, when RNAPII encounters DNA lesions, Set2 can respond rapidly, presumably by methylating H3K36 (77). Previous studies in budding yeast suggest that H3K36me3 recruits Rad26 (Rhp26 in *S. pombe*) through an indirect interaction with Rpd3S subunits (76). Although the direct recruitment of NER factors by H3K36me remains possible, it is unclear if this is the mechanism of action. We found a decrease in the nuclear localization of GFP-tagged Rhp23 in *Δset2* and *H3K36R* cells, as compared with WT cells, which suggests that activation of the NER pathway may be affected. Combining the genetic interaction data and the effect of Set2 on Chk1 activation, the results here suggest that Set2 may act further upstream of NER initiation to sense DNA damage. This is further supported by the effect of Set2 on Rhp23 localization to the *brc1* locus (Figure 4F and G). We noticed that Rhp23 binds more strongly to the *brc1* locus than to the control *act1* locus even in untreated cells (Figure 4F). In case of alkylating damages, the pre-existence of Rhp23 on $brc1^+$ might ensure rapid activation of NER machinery for removal of the damage that interferes with the transcription of DNA damage responsive genes.

The MMS-dependent changes to Rhp23 localization and *brc1* transcription point to a mechanism of rapid activation of NER machineries via the TCR arm upon exposure to alkylation damage at the *brc1* locus; albeit, its remains unclear how the *brc1* locus might be prone to alkylation. Yet, the likelihood of this mechanism is evident through the enrichment of Rhp23 presumably with its interacting partner Rhp41/XPC at sites of damage early after MMS treatment (Figure 4G). Such a prompt response enables repair at a stage when alkylation damage is minimal, and ensures the prompt transcription of the response gene ($brc1^+$) to mount an effective defence against alkylation damage (Supplementary Figure S7B). The promptness of this response is disrupted (but not absent) in *Δset2* cells, which may result in the slower management of alkylating lesions, and obstruction in the timing of the transcription of $brc1^+$ (Supplementary Figure S7A).

Taken together, our observations point to a model whereby Set2 regulates the sensing of alkylation-mediated damage, and full activation of the Chk1 effector checkpoint kinase to further mobilize the TCR factors to coordinate the repair of MMS-dependent aberrations.

H3K36me-dependent Rhp54 foci formation in MMS

Recent studies in yeast suggest that H3K36me influences the choice of repair mechanism through modulation of chromatin structure, without providing any direct role for H3K36me (37,48). Furthermore, in human cells, SETD2-dependent H3K36me3 has been shown to promote HR after DSBs through the recruitment of lens epithelial-derived growth factor p75 (LEDGF) (39), which is found only in metazoans. Here, we define a novel role for Set2 in HR, affecting Rhp54 foci formation possibly through H3K36me in a MMS-dependent manner. When the DNA replication fork is slowed or even stalled following MMS exposure, ssDNA at the fork may be left unrepaired for a much longer time than usual. Such single-stranded regions constitute good substrates for HR, and, if allowed to occur unchecked, will likely lead to a loss of DNA sequences, resulting in genomic instability (78). Consistent with this model, we observed that the replication checkpoint protein Cds1 partially represses the formation of Rhp54 foci, which in turn,

can lead to partial suppression of MMS-induced growth defects arising from a loss of Set2 function (Figure 2C and Supplementary Figure S9). This model further proposes a fine-tuning of HR foci formation as required at different stages of the cell cycle.

The enrichment of H3K36me at sites of DSBs in mammalian cells suggests a potential role of H3K36me in DNA damage sensing and/or repair (38,39). The different forms of H3K36me (di- or tri-) may serve as signals or codes for cells to activate different repair mechanisms; for example, in mammalian cells, H3K36me2 promotes NHEJ whereas H3K36me3 facilitates HR repair (38,39) and precisely localizes the DNA mismatch recognition protein hMutSα onto chromatin (79). In fission yeast, our truncation results suggest that H3K36me3 is the major form of methylation on H3K36 to mediate tolerance to MMS. Furthermore, H3K36me3 may also mediate Rhp23 recruitment to repair alkylation damage at the chromatin via the TCR pathway to safeguard the genome, and we suggest that this may occur via transcriptional control of essential MMS-responsive genes, including *brc1*$^{+}$ (Supplementary Figure S7B). NER may constitute the immediate response to MMS. Its continued presence will then result in persistent damage, which is beyond the capacity of NER to repair and results in the 'back-up plan' of HR-mediated repair. The involvement of Set2 and methylated H3K36 in localizing both Rhp23 and Rhp54 suggests that Set2 may coordinate these repair mechanisms in a timely fashion. However, further experiments will be required to test this hypothesis.

In summary, our study describes the role of Set2 in the DNA damage pathway in response to MMS via the regulation of Chk1 activation. We further show that Set2 acts in NER-mediated repair of alkylation damage and coordinates the timely recruitment of Rhp54 to DNA repair foci.

SUPPLEMENTARY DATA

Supplementary Data are available at NAR Online.

ACKNOWLEDGEMENTS

We thank Rebecca A. Jackson and Joseph Landry for discussion and critically editing the manuscript, Mitsuhiro Yanagida for strains, Liy Sim Low for technical assistance, members of the Chen lab for comments, Nikon Imaging Centre at Biopolis, Singapore, for help with microscopic quantitation of fluorescence signals and intensities. We also thank Jürg Bähler for the opened access tool on his lab website.

Author Contributions: K.K.L. constructed strains and performed all experiments. K.K.L. and Y.P.Y. performed experiments involving Chk1, A.Y.L. performed genetic interactions with *H3K36R*, T.T.T.N. assisted in microscopic analyses, E.S.C. initiated and coordinated the experiments, K.K.L. and E.S.C. wrote the manuscript. All authors approved the submitted version of the manuscript.

FUNDING

Singapore Ministry of Education Academic Research Funds [MOE2016-T2-2-063 awarded to E.S.C.]. Funding for open access charge: Ministry of Education of Singapore [MOE2016-T2-2-063].

Conflict of interest statement. None declared.

REFERENCES

1. Cooke,M.S., Evans,M.D., Dizdaroglu,M. and Lunec,J. (2003) Oxidative DNA damage: mechanisms, mutation, and disease. *FASEB J.*, **17**, 1195–1214.
2. Cecchini,S., Masson,C., La Madeleine,C., Huels,M.A., Sanche,L., Wagner,J.R. and Hunting,D.J. (2005) Interstrand cross-link induction by UV radiation in bromodeoxyuridine-substituted DNA: dependence on DNA conformation. *Biochemistry*, **44**, 16957–16966.
3. Ward,J.F. (1988) DNA damage produced by ionizing radiation in mammalian cells: identities, mechanisms of formation and reparability. Prog. Nucleic Acid Res. Mol. Biol., **35**, 95–125.
4. Ma,W., Westmoreland,J.W., Gordenin,D.A. and Resnick,M.A. (2011) Alkylation base damage is converted into repairable double-strand breaks and complex intermediates in G2 cells lacking AP endonuclease. *PLoS Genet.*, **7**, e1002059.
5. Gasser,S., Zhang,W.Y., Tan,N.Y., Tripathi,S., Suter,M.A., Chew,Z.H., Khatoo,M., Ngeow,J. and Cheung,F.S.G. (2016) Sensing of dangerous DNA. *Mech. Aeging Dev.*, **165**, 33–46.
6. Ciccia,A. and Elledge,S.J. (2010) The DNA damage response: making it safe to play with knives. *Mol. Cell*, **40**, 179–204.
7. You,Z., Chahwan,C., Bailis,J., Hunter,T. and Russell,P. (2005) ATM activation and its recruitment to damaged DNA require binding to the C terminus of Nbs1. *Mol. Cell Biol.*, **25**, 5363–5379.
8. Lee,J.H. and Paull,T.T. (2005) ATM activation by DNA double-strand breaks through the Mre11-Rad50-Nbs1 complex. *Science*, **308**, 551–554.
9. Uziel,T., Lerenthal,Y., Moyal,L., Andegeko,Y., Mittelman,L. and Shiloh,Y. (2003) Requirement of the MRN complex for ATM activation by DNA damage. *EMBO J.*, **22**, 5612–5621.
10. Zou,L. and Elledge,S.J. (2003) Sensing DNA damage through ATRIP recognition of RPA-ssDNA complexes. *Science*, **300**, 1542–1548.
11. Lempiäinen,H. and Halazonetis,T.D. (2009) Emerging common themes in regulation of PIKKs and PI3Ks. *EMBO J.*, **28**, 3067–3073.
12. Cuadrado,M., Martinez-Pastor,B. and Fernandez-Capetillo,O. (2006) ATR activation in response to ionizing radiation: still ATM territory. *Cell Div.*, **1**, 7.
13. Xu,Y.J., Davenport,M. and Kelly,T.J. (2006) Two-stage mechanism for activation of the DNA replication checkpoint kinase Cds1 in fission yeast. *Genes Dev.*, **20**, 990–1003.
14. Limbo,O., Porter-Goff,M.E., Rhind,N. and Russell,P. (2011) Mre11 nuclease activity and Ctp1 regulate Chk1 activation by Rad3^{ATR} and Tel1^{ATM} checkpoint kinases at double-strand breaks. *Mol. Cell Biol.*, **31**, 573–583.
15. Mochida,S., Esashi,F., Aono,N., Tamai,K., O'Connell,M.J. and Yanagida,M. (2004) Regulation of checkpoint kinases through dynamic interaction with Crb2. *EMBO J.*, **23**, 418–428.
16. Baber-Furnari,B.A., Rhind,N., Boddy,M.N., Shanahan,P., Lopez-Girona,A. and Russell,P. (2000) Regulation of mitotic inhibitor Mik1 helps to enforce the DNA damage checkpoint. *Mol. Biol. Cell*, **11**, 1–11.
17. Boddy,M.N., Furnari,B., Mondesert,O. and Russell,P. (1998) Replication checkpoint enforced by kinases Cds1 and Chk1. *Science*, **280**, 909–912.
18. Krogh,B.O. and Symington,L.S. (2004) Recombination proteins in yeast. *Annu. Rev. Genet.*, **38**, 233–271.
19. Johnson,R.D. and Jasin,M. (2000) Sister chromatid gene conversion is a prominent double-strand break repair pathway in mammalian cells. *EMBO J.*, **19**, 3398–3407.
20. Maier,P., Hartmann,L., Wenz,F. and Herskind,C. (2016) Cellular pathways in response to ionizing radiation and their targetability for tumor radiosensitization. *Int. J. Mol. Sci.*, **17**, 102.
21. Lieber,M.R. (2010) NHEJ and its backup pathways in chromosomal translocations. *Nat. Struct. Mol. Biol.*, **17**, 393–395.
22. Featherstone,C. and Jackson,S.P. (1999) DNA double-strand break repair. *Curr. Biol.*, **9**, R759–R761.
23. Carter,R.J. and Parsons,J.L. (2016) Base excision repair, a pathway regulated by posttranslational modifications. *Mol. Cell Biol.*, **36**, 1426–1437.

24. Kanamitsu,K. and Ikeda,S. (2010) Early steps in the DNA base excision repair pathway of a fission yeast *Schizosaccharomyces pombe*. *J. Nucleic Acids*, **2010**, 1–9.
25. Kondo,N., Takahashi,A., Ono,K. and Ohnishi,T. (2010) DNA damage induced by alkylating agents and repair pathways. *J. Nucleic Acids*, **2010**, 543531.
26. Memisoglu,A. and Samson,L. (2000) Base excision repair in yeast and mammals. *Mutat. Res.*, **451**, 39–51.
27. Lombaerts,M., Peltola,P.H., Visse,R., den Dulk,H., Brandsma,J.A. and Brouwer,J. (1999) Characterization of the rhp7(+) and rhp16(+) genes in *Schizosaccharomyces pombe*. *Nucleic Acids Res.*, **27**, 3410–3416.
28. Fousteri,M., Vermeulen,W., van Zeeland,A.A. and Mullenders,L.H. (2006) Cockayne syndrome A and B proteins differentially regulate recruitment of chromatin remodeling and repair factors to stalled RNA polymerase II in vivo. *Mol. Cell*, **23**, 471–482.
29. Sugasawa,K., Okamoto,T., Shimizu,Y., Masutani,C., Iwai,S. and Hanaoka,F. (2001) A multistep damage recognition mechanism for global genomic nucleotide excision repair. *Genes Dev.*, **15**, 507–521.
30. Li,S. (2015) Transcription coupled nucleotide excision repair in the yeast *Saccharomyces cerevisiae*: the ambiguous role of Rad26. *DNA Repair (Amst.)*, **36**, 43–48.
31. Li,W., Selvam,K., Rahman,S.A. and Li,S. (2016) Sen1, the yeast homolog of human senataxin, plays a more direct role than Rad26 in transcription coupled DNA repair. *Nucleic Acids Res.*, **44**, 6794–6802.
32. de Laat,W.L., Jaspers,N.G.J. and Hoeijmakers,J.H.J. (1999) Molecular mechanism of nucleotide excision repair. *Genes Dev.*, **13**, 768–785.
33. Staresincic,L., Fagbemi,A.F., Enzlin,J.H., Gourdin,A.M., Wijgers,N., Dunand-Sauthier,I., Giglia-Mari,G., Clarkson,S.G., Vermeulen,W. and Schärer,O.D. (2009) Coordination of dual incision and repair synthesis in human nucleotide excision repair. *EMBO J.*, **28**, 1111–1120.
34. Paul-Konietzko,K., Thomale,J., Arakawa,H. and Iliakis,G. (2015) DNA ligases I and III support nucleotide excision repair in DT40 cells with similar efficiency. *J. Photochem. Photobiol.*, **91**, 1173–1180.
35. Mocquet,V., Lainé,J.P., Riedl,T., Yajin,Z., Lee,M.Y. and Egly,J.M. (2008) Sequential recruitment of the repair factors during NER: the role of XPG in initiating the resynthesis step. *EMBO J.*, **27**, 155–167.
36. Kim,H.S., Rhee,D.K. and Jang,Y.K. (2008) Methylations of histone H3 lysine 9 and lysine 36 are functionally linked to DNA replication checkpoint control in fission yeast. *Biochem. Biophys. Res. Commun.*, **368**, 419–425.
37. Pai,C.C., Deegan,R.S., Subramanian,L., Gal,C., Sarkar,S., Blaikley,E.J., Walker,C., Hulme,L., Bernhard,E., Codlin,S. *et al.* (2014) A histone H3K36 chromatin switch coordinates DNA double-strand break repair pathway choice. *Nat. Commun.*, **5**, 4091.
38. Fnu,S., Williamson,E.A., De Haro,L.P., Brenneman,M., Wray,J., Shaheen,M., Radhakrishnan,K., Lee,S.H., Nickoloff,J.A. and Hromas,R. (2011) Methylation of histone H3 lysine 36 enhances DNA repair by nonhomologous end-joining. *Proc. Natl. Acad. Sci. U.S.A.*, **108**, 540–545.
39. Pfister,S.X., Ahrabi,S., Zalmas,L.P., Sarkar,S., Aymard,F., Bachrati,C.Z., Helleday,T., Legube,G., La Thangue,N.B., Porter,A.C. and Humphrey,T.C. (2014) SETD2-dependent histone H3K36 trimethylation is required for homologous recombination repair and genome stability. *Cell Rep.*, **7**, 2006–2018.
40. Forsburg,S.L. and Rhind,N. (2006) Basic methods for fission yeast. *Yeast*, **23**, 173–183.
41. Moreno,S., Klar,A. and Nurse,P. (1991) Molecular genetic analysis of fission yeast *Schizosaccharomyces pombe*. *Methods Enzymol.*, **194**, 795–823.
42. Nguyen,T.T., Lim,J.S., Tang,R.M., Zhang,L. and Chen,E.S. (2015) Fitness profiling links topoisomerase II regulation of centromeric integrity to doxorubicin resistance in fission yeast. *Sci. Rep.*, **5**, 8400.
43. Tay,Z., Eng,R.J., Sajiki,K., Lim,K.K., Tang,M.Y., Yanagida,M. and Chen,E.S. (2013) Cellular robustness conferred by genetic crosstalk underlies resistance against chemotherapeutic drug doxorubicin in fission yeast. *PLoS ONE*, **8**, e55041.
44. Nguyen,T.T., Chua,J.K., Seah,K.S., Koo,S.H., Yee,J.Y., Yang,E.G., Lim,K.K., Pang,S.Y., Yuen,A., Zhang,L. *et al.* (2016) Predicting chemotherapeutic drug combinations through gene network profiling. *Sci. Rep.*, **6**, 18658.
45. Li,M., Phatnani,H.P., Guan,Z., Sage,H., Greenleaf,A.L. and Zhou,P. (2005) Solution structure of the Set2-Rpb1 interacting domain of human Set2 and its interaction with the hyperphosphorylated C-terminal domain of Rpb1. *Proc. Natl. Acad. Sci. U.S.A.*, **102**, 17636–17641.
46. Volland,C., Urban-Grimal,D., Géraud,G. and Haguenauer-Tsapis,R. (1994) Endocytosis and degradation of the yeast uracil permease under adverse conditions. *J. Biol. Chem.*, **269**, 9833–9841.
47. Lim,K.K., Ong,T.Y., Tan,Y.R., Yang,E.G., Ren,B., Seah,K.S., Yang,Z., Tan,T.S., Dymock,B.W. and Chen,E.S. (2015) Mutation of histone H3 serine 86 disrupts GATA factor Ams2 expression and precise chromosome segregation in fission yeast. *Sci. Rep.*, **5**, 14064.
48. Jha,D.K. and Strahl,B.D. (2014) An RNA polymerase II-coupled function for histone H3K36 methylation in checkpoint activation and DSB repair. *Nat. Commun.*, **5**, 3965.
49. Stracker,T.H., Usui,T. and Petrini,J.H. (2009) Taking the time to make important decisions: the checkpoint effector kinases Chk1 and Chk2 and the DNA damage response. *DNA Repair (Amst.)*, **8**, 1047–1054.
50. Matsuura,A., Naito,T. and Ishikawa,F. (1999) Genetic control of telomere integrity in *Schizosaccharomyces pombe*: rad3(+) and tel1(+) are parts of two regulatory networks independent of the downstream protein kinases chk1(+) and cds1(+). *Genetics*, **152**, 1501–1512.
51. Parrilla-Castellar,E.R., Arlander,S.J. and Karnitz,L. (2004) Dial 9-1-1 for DNA damage: the Rad9-Hus1-Rad1 (9-1-1) clamp complex. *DNA Repair (Amst.)*, **3**, 1009–1014.
52. Lopez-Girona,A., Tanaka,K., Chen,X.B., Baber,B.A., McGowan,C.H. and Russell,P. (2001) Serine-345 is required for Rad3-dependent phosphorylation and function of checkpoint kinase Chk1 in fission yeast. *Proc. Natl. Acad. Sci. U.S.A.*, **98**, 11289–11294.
53. Shimada,K., Pasero,P. and Gasser,S.M. (2002) ORC and the intra-S-phase checkpoint: a threshold regulates Rad53p activation in S phase. *Genes Dev.*, **16**, 3236–3252.
54. Chahwan,C., Nakamura,T.M., Sivakumar,S., Russell,P. and Rhind,N. (2003) The fission yeast Rad32 (Mre11)-Rad50-Nbs1 complex is required for the S-phase DNA damage checkpoint. *Mol. Cell Biol.*, **23**, 6564–6573.
55. Porter-Goff,M.E. and Rhind,N. (2009) The role of MRN in the S-phase DNA damage checkpoint is independent of its Ctp1-dependent roles in double-strand break repair and checkpoint signaling. *Mol. Biol. Cell*, **20**, 2096–2107.
56. Furnari,B., Rhind,N. and Russell,P. (1997) Cdc25 mitotic inducer targeted by chk1 DNA damage checkpoint kinase. *Science*, **277**, 1495–1497.
57. O'Connell,M.J., Raleigh,J.M., Verkade,H.M. and Nurse,P. (1997) Chk1 is a wee1 kinase in the G2 DNA damage checkpoint inhibiting cdc2 by Y15 phosphorylation. *EMBO J.*, **16**, 545–554.
58. Maki,K., Inoue,T., Onaka,A., Hashizume,H., Somete,N., Kobayashi,Y., Murakami,S., Shigaki,C., Takahashi,T.S., Masukata,H. and Nakagawa,T. (2011) Abundance of prepreplicative complexes (Pre-RCs) facilitates recombinational repair under replication stress in fission yeast. *J. Biol. Chem.*, **286**, 41701–41710.
59. Sakurai,E., Susuki,M., Kanamitsu,K., Kawano,S. and Ikeda,S. (2015) Global genome nucleotide excision repair proteins Rhp7p and Rhp41p are involved in abasic site repair of *Schizosaccharomyces pombe*. *Adv. Biosci. Biotech.*, **6**, 265–274.
60. Alseth,I., Osman,F., Korvald,H., Tsaneva,I., Whitby,M.C., Seeberg,E. and Bjørås,M. (2005) Biochemical characterization and DNA repair pathway interactions of Mag1-mediated base excision repair in *Schizosaccharomyces pombe*. *Nucleic Acids Res.*, **33**, 1123–1131.
61. Kanamitsu,K., Tanihigashi,H., Tanita,Y., Inatani,S and Ikeda,S. (2007) Involvement of 3-methyladenine DNA glycosylases Mag1p and Mag2p in base excision repair of methyl methanesulfonate-damaged DNA in the fission yeast *Schizosaccharomyces pombe*. *Genes Genet. Syst.*, **82**, 489–494.
62. Lombaerts,M., Goeloe,J.I., den Dulk,H., Brandsma,J.A. and Brouwer,J. (2000) Identification and characterization of the rhp23(+) DNA repair gene in *Schizosaccharomyces pombe*. *Biochem. Biophys. Res. Commun.*, **268**, 210–215.
63. Memisoglu,A. and Samson,L. (2000) Contribution of base excision repair, nucleotide excision repair, and DNA recombination to alkylation resistance of the fission yeast *Schizosaccharoyces pombe*. *J. Bacteriol.*, **182**, 2104–2112.

64. Kanamitsu,K. and Ikeda,S. (2011) Fission yeast homologs of human XPC and CSB, *rhp41* and *rhp26*, are involved in transcription-coupled repair of methyl methanesulfonate-induced DNA damage. *Genes Genet. Syst.*, **86**, 83–91.
65. Latypov,V.F., Tubbs,J.L., Watson,A.J., Marriott,A.S., McGown,G., Thorncroft,M., Wilkinson,O.J., Senthong,P., Butt,A., Arvai,A.S. *et al.* (2012) Atl1 regulates choice between global genome and transcription-coupled repair of O^6-alkylguanines. *Mol. Cell*, **47**, 50–60.
66. Heinen,C., Ács,K., Hoogstraten,D. and Dantuma,N.P. (2011) C-terminal UBA domains protect ubiquitin receptors by preventing initiation of protein degradation. *Nat. Commun.*, **2**, 191.
67. Movsichoff,F., Castro,O.A. and Parodi,A.J. (2005) Characterization of *Schizosaccharomyces pombe* ER α-Mannosidase: A reevaluation of the role of the enzyme on ER-associated degradation. *Mol. Biol. Cell*, **16**, 4714–4724.
68. Kitamura,K. and Fujiwara,H. (2013) The type-2 N-end rule peptide recognition activity of Ubr11 ubiquitin ligase is required for the expression of peptide transporters. *FEBS Lett*, **587**, 214–219.
69. Chen,D., Toone,W.M., Mata,J., Lyne,R., Burns,G., Kivinen,K., Brazma,A., Jones,N. and Bähler,J. (2003) Global transcriptional responses of fission yeast to environmental stress. *Mol. Biol. Cell*, **14**, 214–229.
70. Sheedy,D.M., Dimitrova,D., Rankin,J.K., Bass,K.L., Lee,K.M., Tapia-Alveal,C., Harvey,S.H., Murray,J.M. and O'Connell,M.J. (2005) Brc1-mediated DNA repair and damage tolerance. *Genetics*, **171**, 457–468.
71. Williams,J.S., Williams,R.S., Dovey,C.L., Guenther,G., Tainer,J.A. and Russell,P. (2010) gammaH2A binds Brc1 to maintain genome integrity during S-phase. *EMBO J.*, **29**, 1136–1148.
72. Ferreira,M.G. and Cooper,J.P. (2004) Two modes of DNA double-strand break repair are reciprocally regulated through the fission yeast cell cycle. *Genes Dev.*, **18**, 2249–2254.
73. Downs,J.A. and Jackson,S.P. (2004) A means to a DNA end: the many roles of Ku. *Nat. Rev. Mol. Cell Biol.*, **5**, 367–378.
74. Gasch,A.P., Huang,M., Metzner,S., Botstein,D., Elledge,S.J. and Brown,P.O. (2001) Genomic expression responses to DNA-damaging agents and the regulatory role of the yeast ATR homolog Mec1p. *Mol. Biol. Cell*, **12**, 2987–3003.
75. Cao,L.L., Wei,F., Du,Y., Song,B., Wang,D., Shen,C., Lu,X., Cao,Z., Yang,Q., Gao,Y. *et al.* (2016) ATM-mediated KDM2A phosphorylation is required for the DNA damage repair. *Oncogene*, **35**, 301–313.
76. Malik,S., Chaurasia,P., Lahudkar,S., Durairaj,G., Shukla,A. and Bhaumik,S.R. (2010) Rad26p, a transcription-coupled repair factor, is recruited to the site of DNA lesion in an elongating RNA polymerase II-dependent manner in vivo. *Nucleic Acids Res.*, **38**, 1461–1477.
77. Landry,J., Sutton,A., Hesman,T., Min,J., Xu,R.M., Johnston,M. and Sternglanz,R. (2003) Set2-catalyzed methylation of histone H3 represses basal expression of GAL4 in *Saccharomyces cerevisiae*. *Mol. Cell Biol.*, **23**, 5972–5978.
78. Kadyk,L.C. and Hartwell,L.H. (1993) Replication-dependent sister chromatid recombination in rad1 mutants of *Saccharomyces cerevisiae*. *Genetics*, **133**, 469–487.
79. Li,F., Mao,G., Tong,D., Huang,J., Gu,L., Yang,W. and Li,G. (2013) The histone mark H3K36me3 regulates human DNA mismatch repair through its interaction with MutSα. *Cell*, **153**, 590–600.